The CSPD-1 γ-Ray Vision System

Z. He, J. Obermark[†], J. Du, D.K. Wehe, S.W. Lee[†], G.F. Knoll
Nuclear Engineering Department,
[†]Electrical Engineering and Computer Science Department,
The University of Michigan,
Ann Arbor, MI 48109, U.S.A.

Abstract

The CSPD-1 γ-ray vision system has been constructed for the energy range from 100 keV up to a few MeV, which encompasses most energies of γ-ray radiation from the radioactive nuclides of interest to nuclear facilities. The angular resolution of the system can be varied from about 7° down to 3° FWHM. The energy resolution at 662 keV is 6.8% or 8.9% FWHM depending on which of the two detectors are used. The detected spatial distribution of γ-rays is overlayed with the video image taken from a small CCD camera mounted on the side of the collimator. This enables immediate localization of the radioactive area. Some results obtained at the Molten Salt Reactor Experiment (MSRE) at the Oak Ridge National Laboratory (ORNL) are reported, and recommended improvements are discussed.

I. INTRODUCTION

Portable γ-ray detectors with imaging capability in the energy range of 100 keV to a few MeV are required for a number of applications in the nuclear industry, such as radiation monitoring in nuclear power plants, radioactivity distribution measurements for nuclear material inspections, and radiation surveillance in decontamination activities.

Many γ-ray imaging techniques have been developed over the past three decades. Spatially modulated coded-masks [1, 2] have been extensively employed in γ-ray astronomy due to their high detection efficiency and superior performance over conventional collimators for point sources, but are not attractive for distributed sources. Time modulated coded-masks [3, 4, 5] were explored in medical γ-ray tomography. Compton-scatter γ-ray imagers have been used in astronomy [6] and investigated for radiation monitoring [7], but are also not yet practical for a portable radiation imaging system. Pinhole collimators [8, 9] and diverging multi-hole collimators [10] remain the practical choices for compact systems. However, the use of pinhole collimators is limited to the energy range below 1 MeV. This is because the pinhole becomes ineffective for high energy γ-rays, and it is difficult to obtain sufficiently good position resolution on the γ-ray detector.

Following our previous works [11, 12, 10], a portable γ-ray imager CSPD-1 has been developed which can superimpose the detected γ-ray distribution onto a video image taken from a small CCD camera mounted on the side of the collimator. The γ-ray image can be processed by a maximum-likelihood image reconstruction algorithm. The reconstruction provides a more accurate estimation of the γ-ray distribution by taking into account the point response function of the system. Imaging has been performed at the Molten Salt Reactor Experiment at the ORNL, and some of the results are reported here.

II. SYSTEM DESIGN

The system was constructed based on the prototype device previously reported [10]. The collimator is made of two layers of lead disks having 1 inch thickness due to the cost and ready availability of the material. The front collimator disk can be rotated along its axis and is accurately controlled by a stepping motor. Both layers of the collimator have one 6 mm square aperture. Since both apertures are located 2 cm from the centers of the disks, the signal and background observations can be carried out by aligning the two apertures and then rotating the aperture on the front collimator to the opposite side. The separation between the two layers of collimators can be smoothly adjusted to vary the field of view from about 7° FWHM down to 3° FWHM. This type of collimator was chosen because the sensitivity of the system can be maintained while changing the angular resolution and it can be constructed using thick material for enhanced background suppression. These conditions are required for good angular resolution at high γ-ray energies while achieving a good detection efficiency.

Incident γ-rays passing through the aperture (as well as those penetrating the shield) are detected by a single γ-ray detector. Two CsI(Tl)/photodiode detectors [13] have been investigated for the γ-ray detection. The first detector is a 1×1×2.5 cm CsI(Tl) coupled to a 1 cm^2 PIN silicon photodiode. The second detector is a 2.5 cm in diameter and 2.5 cm long CsI(Tl) coupled to a 1 cm^2 photodiode. Their outside dimensions, with the preamplifier

*This work was supported under the U.S. Department of Energy, Robotics for Hazardous Environments, Grant No. DOE-FG02-86NE37969.

sealed inside its housing, are 1.5×1.5×6.8 cm and 3.8 cm ϕ by 8.1 cm long respectively. The first detector is for the energy range below 1.5 MeV and the second detector was ordered for the higher energy γ-rays encountered in some field tests at the MSRE. CsI(Tl)/photodiode detectors were chosen for their compactness, ruggedness, good stopping power for γ-rays, competitive energy resolution at energies above 500 keV, low voltage requirements and insensitivity to external magnetic fields. This latter factor can be important for a portable device.

A small CCD camera with outside dimensions of 4×4×6.5 cm is mounted on the edge of the supporting frame of the collimator. The center of the field of view of the optical camera is parallel to the aligned axis of the two apertures of the collimator.

The γ-ray detector is shielded by 2.5 cm thick lead on all sides (except the bottom to permit easily swapping detectors). The collimator, CCD camera and γ-ray detector are mounted on a pan-and-tilt table which can be rotated in two dimensions and controlled by a 486 PC. By pointing the detector in different directions, the γ-ray distribution in two dimensions can be mapped. After the observation, the γ-ray image is superimposed onto the video image taken from the CCD camera for identifying the origin of the γ-ray emission.

III. Spectroscopy Performance

The energy resolution of the 1×1×2.5 cm CsI(Tl) detector was obtained at several γ-ray energies and the results are summarized in Figure 1. One can see that the low energy threshold is about 40 keV on this detector. The larger CsI(Tl) detector, which is 2.5 cm in diameter and 2.5 cm long, has a poorer energy resolution of 8.9% at 662 keV and a higher low energy threshold at about 100 keV. This is mainly caused by the lower light collection efficiency of a 1 cm^2 photodiode on the larger area crystal. However, the larger detector has a better photo-peak efficiency for high energy γ-rays. Both of these two detectors were manufactured by Vela Limited of the U.K. [13].

IV. Spatial Resolution

The angular resolution of the system is mainly defined by the field of view of the aperture of the collimator. Since the area of the apertures of the collimator are fixed at 6×6 mm, increasing the separation of the two layers of the lead disks varies the angular resolution from 7° down to 3° FWHM. The angular resolution is poorer at higher γ-ray energies due to the penetration of γ-rays. Because of the limited spatial resolution, the observed γ-ray distribution is a convolution of the true γ-ray distribution with the point response function of the system. The true source distribution can be estimated using a maximum-likelihood image reconstruction algorithm [14] that includes the knowledge of the response of the system as a function of incident γ-ray direction. This was demonstrated [10] using a point ^{137}Cs source.

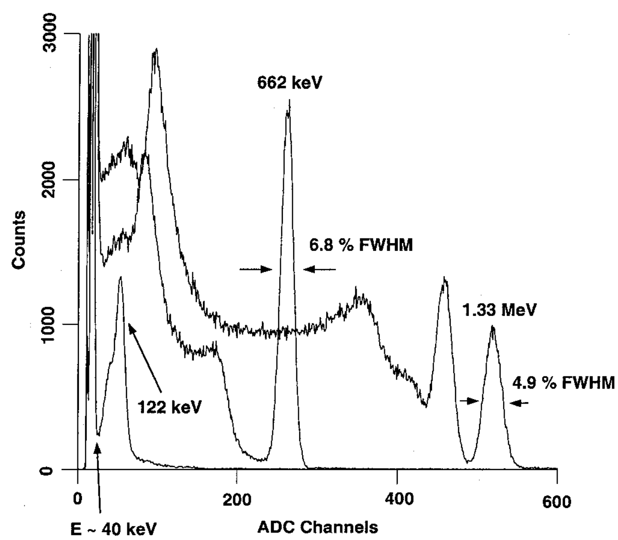

Figure 1: Energy spectra of the 1×1×2.5 cm CsI(Tl) detector at room temperature.

In order to test whether this reconstruction algorithm is as effective on extended sources, an irradiated nickel ring which emits γ-rays at 811 keV was imaged. The diameter of the nickel ring was 6.5 cm and it was located 50 cm from the camera. As a result, the nickel ring subtends an annular diameter of 7.4° towards the camera. The raw image and the reconstructed distribution of γ-rays are shown in Figures 2 (a) and (b) respectively for comparison. The field of view of both images are 17×17 degrees. The camera scan step was 1°/observation. The pixel size of the reconstructed image was chosen to be 0.5° in order to show the structure of the reconstructed nickel ring. In this experiment, the geometrical FWHM of the field of view of the aperture was set to be 3°, which should be the spatial resolution at low γ-ray energies. The effective angular resolution at 811 keV is estimated to be about 4° FWHM. Comparing Figures 2 (a) and (b), it is evident that the image quality can be greatly enhanced through the image reconstruction process. The radioactivity of the nickel ring was about one hundred millicurie and the observation time was 20 seconds at each pointing direction. The observed signal-to-noise ratio was high due to the intense activity of the source.

V. Observations at ORNL

Some contaminated areas in the MSRE at ORNL were imaged using this portable γ-ray imaging system. The primary interest was to identify the distribution of the fission product ^{137}Cs (662 keV γ-rays), and ^{208}Tl (2.6 MeV γ-rays) which is a daughter in the ^{232}U decay chain. The

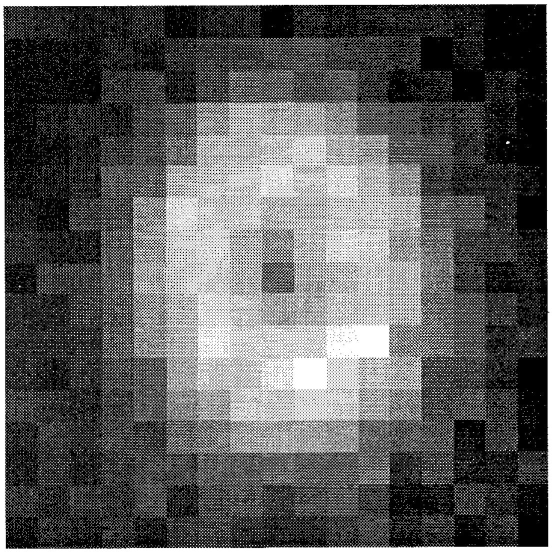

(a) The raw image

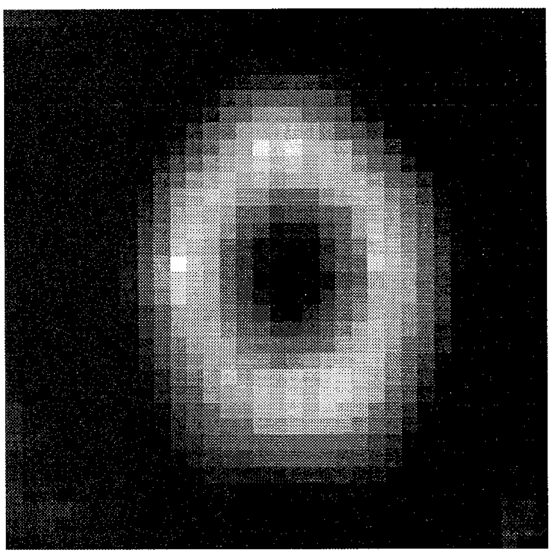

(b) Reconstructed image using MLEM

Figure 2: Image obtained at 811 keV. The nickel ring subtends an annular ring of 7.4° in diameter.

typical observation time was one minute at each pointing direction and about ten hours for a whole scan. This provides a γ-ray intensity distribution over a field of view of 40×40 degrees. The geometrical FWHM of the field of view of the aperture was set to be 4° during all measurements. The typical background dose rate at the camera was ~ 2-3 mR/h, with a significant contribution from the 2.6 MeV γ-rays and the Compton scattered photons.

The net γ-ray signal N_s observed at each pointing direction was obtained by:

$$N_s = N_{open} - N_{close} \qquad (1)$$

where N_{open} and N_{close} are the number of photons detected when the aperture of the collimator were open and closed respectively. Since both N_{open} and N_{close} were usually much bigger than 100 during our measurements, the Gaussian distribution can be used to describe the statistical behavior of these two variables. Therefore, the variance of N_s can be obtained using:

$$\sigma(N_s) = \sqrt{N_{open} + N_{close}} \qquad (2)$$

and the signal-to-noise ratio (SNR) of the observed signal can be calculated using $SNR = N_s/\sigma(N_s)$. The γ-ray signals are superimposed on to the video image only when the corresponding $SNR \geq 2.5$.

The observed ^{137}Cs and ^{208}Tl images at the lower half of the Sampler-Enricher at the MSRE are shown in Figures 3 (a) and (b) respectively. The field of view of the images is 40×40 degrees and the scan step was 2°. It was surprising that the distribution of ^{137}Cs was different from that of ^{208}Tl.

Another MSRE image is shown in Figure 4. The field of view and the scan step were the same as that in Figure 3. ^{208}Tl deposition was clearly identified at the valve on a horizontal pipe. ^{137}Cs was not seen at the valve although it was common at other locations. The angular resolution of the system at 2.6 MeV is difficult to obtain in the laboratory a priori due to the unavailability of common γ-ray sources at such high energy. In Figure 4, the dimension of the valve is ~ 2° wide, which is small compared with the geometrical FWHM of the field of view of the aperture of 4°. Therefore, one can estimate that the angular resolution of the device is ~ 5° FWHM at the 2.6 MeV γ-ray energy. This precision would be very difficult to achieve by using other types of mechanically collimated apertures. The detected number of background γ-rays at each pointing direction varied from ~520 to ~1050 at 2.6 MeV. Without subtraction of the background using the rotation aperture on the front lead disk of the collimator, the γ-ray source at the valve would not have been identified.

These images have provided valuable information on the location of radioactive materials and will help in the decommissioning process to ultimately dismantle the facility.

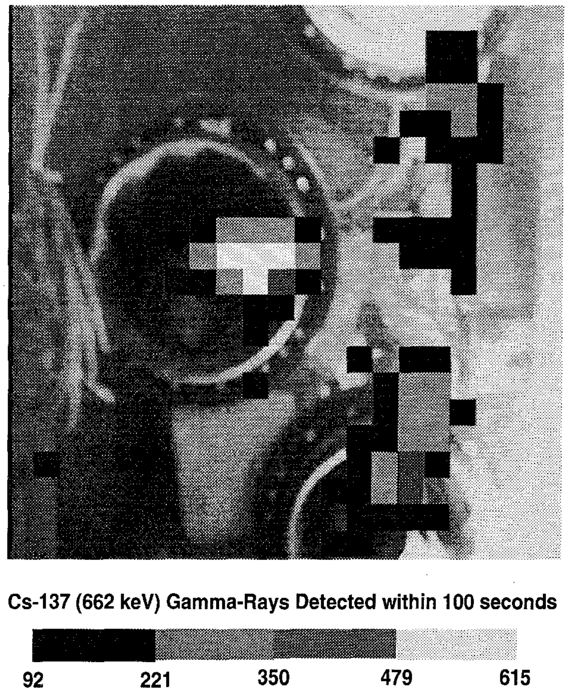

(a) The image of ^{137}Cs (662 keV).

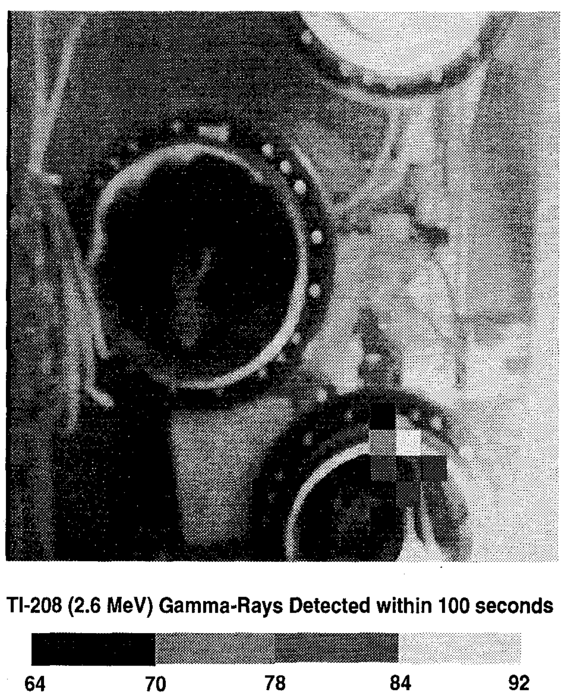

(b) The image of ^{208}Tl (2.6 MeV).

Figure 3: γ-ray images obtained at the Sampler-Enricher of MSRE.

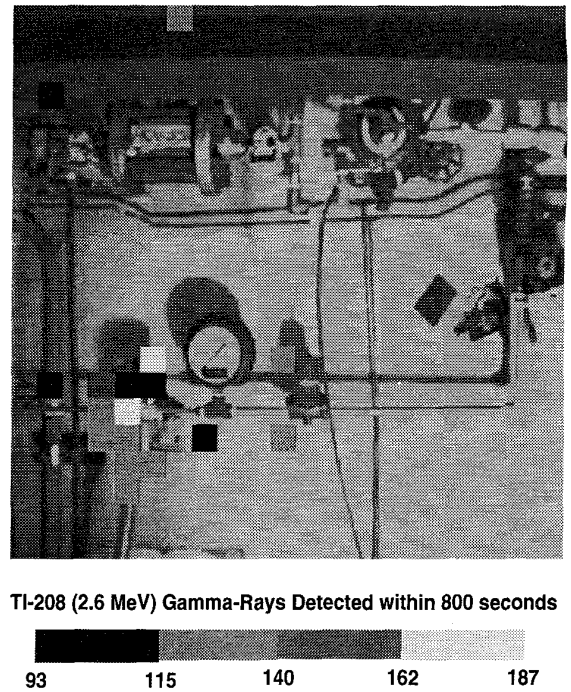

Figure 4: A γ-ray image obtained at MSRE of ORNL.

VI. Future Improvements

In order to reduce the measurement time and to increase the sensitivity, a detector array was constructed for us by eV Products. It consists of 16 1×1×3 cm CsI(Tl) scintillation crystals coupled to 1 cm^2 Hamamatsu photodiodes. Detectors and preamplifiers are integrated inside one housing with outside dimensions of 7.8×8.3×8.5 cm. Each individual detector can operate as an active veto shield to its neighboring detectors in order to reduce the background and to increase the photopeak-to-Compton ratio. The energy resolutions of the detectors have been tested at 662 keV γ-ray energy. Twelve detectors ranged from 6.5% to 7.3% FWHM, but four detectors had poorer resolutions ranging from 7.6% to 8.6% FWHM. The use of this detector array will greatly increase the detection efficiency and reduce imaging time proportionally. Different collimators, such as pinhole collimators, multi-hole collimators or coded masks, can be used interchangeably with this detector array. This will enable us to obtain the optimized performance for different γ-ray spatial and energy distributions.

VII. Conclusions

A portable γ-ray imaging system has been constructed and measurements have been carried out at field sites. Good spectral and spatial resolution has been demonstrated at γ-ray energies up to 2.6 MeV. Its ability of superimpose the γ-ray distribution onto a video image can expedite identifying radioactive locations, some of which might not otherwise be identified using non-imaging detectors. The use of this device has already provided valuable help in a DOE decommissioning project at ORNL. The sensitivity of the current system will be significantly increased with a new 16 cell detector array.

VIII. Acknowledgments

The authors are grateful to M.A. Buckner and V.C. Miller of the Oak Ridge National Laboratory for their help in the measurements at the MSRE.

IX. References

[1] E.E. Fenimore & T.M. Cannon, "Coded aperture imaging with uniformly redundant arrays", *Applied Optics*, vol. 17(3), pp. 337–347, 1978.

[2] W.R. Cook et al., "Gamma-ray imaging with a rotation hexagonal uniformly redundant array", *IEEE Transactions on Nuclear Science*, vol. 31(1), pp. 771–775, 1984.

[3] G.F. Knoll et al., "Pseudorandom filters and correlation analysis applied to gamma ray imaging", *Journal of Nuclear Medicine*, vol. 15, pp. 507, 1974.

[4] R.S. May et al., "Gamma-ray imaging with stochastic apertures", *Applied Optics*, vol. 13(11), pp. 2589–2601, 1974.

[5] W.L. Rogers et al., "Coded-aperture imaging of the heart", *Journal of Nuclear Medicine*, vol. 21(4), pp. 371–378, 1980.

[6] P.von Ballmoos et al., "Imaging the gamma-ray sky with Compton telescope", *Astronomy and Astrophysics*, vol. 221, pp. 396–406, 1989.

[7] J.B. Martin et al., "Imaging multi-energy γ-ray fields with a Compton scatter camera", *IEEE Transactions on Nuclear Science*, vol. 41, pp. 1019–1025, 1994.

[8] R.H. Redus et al., "A combined video and gamma ray imaging system for robots in nuclear environments", *Nuclear Instruments and Methods*, vol. A353, pp. 324–327, 1994.

[9] A.N. Sudarkin et al., "HERV - high energy radiation visualizer, a new system for imaging in x-ray and gamma regions", *Conference Record of 1994 IEEE Nuclear Science Symposium and Medical Imaging Conference, Norfolk, Virginia. Oct.30 - Nov.5, 1994.*

[10] Z. He et al., "Portable wide-angle γ-ray vision systems", *IEEE Transactions on Nuclear Science*, vol. 42(4), pp. 668–674, 1995.

[11] T.A. DeVol et al., "Gamma-ray spectral imaging using a single-shutter radiation camera", *Nuclear Instruments and Methods*, vol. A299, pp. 495–500, 1990.

[12] S.V. Guru et al., "A portable gamma camera for radiation monitoring", *IEEE Transactions on Nuclear Science*, vol. 42(4), pp. 940–945, 1995.

[13] Vela Limited, "Technical Notes of Vela Radiation Detection System", *29 St. Mary's road, Southampton, U.K.* .

[14] K. Lange & R. Carson, "EM reconstruction algorithms for emission and transmission tomography", *Journal of Computer Assisted Tomography*, vol. 8(2), pp. 306–316, 1984.